



HAL
open science

A broadband method for liner impedance eduction in the presence of a mean flow

Renata Troian, Didier Dragna, Christophe Bailly, Marie-Annick Galland

► **To cite this version:**

Renata Troian, Didier Dragna, Christophe Bailly, Marie-Annick Galland. A broadband method for liner impedance eduction in the presence of a mean flow. CFM 2015 - 22ème Congrès Français de Mécanique, Aug 2015, Lyon, France. hal-03446549

HAL Id: hal-03446549

<https://hal.science/hal-03446549>

Submitted on 24 Nov 2021

HAL is a multi-disciplinary open access archive for the deposit and dissemination of scientific research documents, whether they are published or not. The documents may come from teaching and research institutions in France or abroad, or from public or private research centers.

L'archive ouverte pluridisciplinaire **HAL**, est destinée au dépôt et à la diffusion de documents scientifiques de niveau recherche, publiés ou non, émanant des établissements d'enseignement et de recherche français ou étrangers, des laboratoires publics ou privés.

A broadband method for liner impedance eduction in the presence of a mean flow

R. TROIAN^a,
D. DRAGNA^b,
C. BAILLY^c,
M.-A. GALLAND^d,

a. renata.troian@ec-lyon.fr

b. didier.dragna@ec-lyon.fr

c. christophe.bailly@ec-lyon.fr

d. marie-annick.galland@ec-lyon.fr

Laboratoire de Mécanique des Fluides et d'Acoustique, UMR CNRS 5509, École Centrale de Lyon,
36, avenue Guy de Collongue, 69134 Écully Cedex, France

Abstract :

In this study, a broadband impedance eduction method is developed to identify the surface impedance of acoustic liners, mounted in the walls of aircraft engine nacelles, from measurements on a test rig. A numerical model of an acoustic liner under a grazing flow is undertaken by considering finite-difference time-domain simulations and the Euler equations for the acoustic propagation. A broadband impedance model is used to prescribe time-domain boundary conditions. The impedance eduction procedure is established using an multiobjective optimization with the genetic algorithm NSGA-II. The pressure is measured at six positions in the duct for each considered frequency. The present methodology is validated by comparison with benchmark data provided by NASA.

Key words : impedance eduction; acoustic propagation; finite difference time domain modeling; broadband impedance model; multiobjective optimization

1 Introduction

Acoustic liners mounted in the walls of aircraft engine nacelles are commonly used to achieve noise reduction. Due to the increase of the engine size to obtain ultra-high by-pass ratio, the size of nacelles is expected to be shortened in the next generation of aircrafts and consequently, the efficiency of current liners will decrease as well. The key parameter to evaluate noise reduction of novel concepts is the surface impedance of the liners. To determine it in situ, inverse techniques based on propagation models for the lined duct are becoming popular because of their convenience and advantages. These methods are performed through the measurement of the acoustic pressure at selected locations outside the liner and have an extra advantage of not destroying the liner sample.

For indirect impedance eduction at least two different steps must be carried out. First, the acoustic propagation in the lined duct for a given geometry of the liner must be simulated. Second, an impedance eduction method based on experimental inputs have to be developed.

In order to model the acoustic propagation under the grazing flow several approaches were proposed. Approaches based on linearized Euler equations resolution use the finite element [14, 7, 6, 8] or the finite-difference method [9, 10] for numerical simulations. Helmholtz equations are also considered in the mode matching models [5, 12].

In the present study the linearized Euler equations are solved using finite-difference time-domain (FDTD) techniques, and a time-domain impedance boundary condition is implemented. The acoustic impedance characteristics are obtained with the iterative impedance eduction method, that consists in minimizing the error between the numerically calculated and the measured sound pressure along the duct.

The paper is organized as follows. The numerical modelling of the acoustic propagation under the grazing flow of a rectangular lined duct together with impedance boundary condition is discussed in Section 2. The impedance eduction method is presented in Section 3. The method is then validated by comparison with experimental data from the NASA Langley Research Center Grazing Incidence Tube, and results are presented in Section .

2 Modeling of acoustic propagation

2.1 Linearized Euler equations

Sound propagation in lined duct is governed by the linearized Euler equations (LEEs), obtained by linearization of the Euler equations around a given mean flow of density ρ_0 and velocity \mathbf{V}_0 . The mean pressure is assumed to be constant. The acoustic velocity \mathbf{v} and the acoustic pressure p are given by

$$\frac{\partial p}{\partial t} + (\mathbf{V}_0 \cdot \nabla) p + \rho_0 c_0^2 \nabla \cdot \mathbf{v} = 0, \quad (1)$$

$$\frac{\partial \mathbf{v}}{\partial t} + (\mathbf{V}_0 \cdot \nabla) \mathbf{v} + (\mathbf{v} \cdot \nabla) \mathbf{V}_0 + \frac{1}{\rho_0} \nabla p = 0. \quad (2)$$

where t is the time and c_0 is the speed of sound in air. The linearized Euler equations are solved using low-dispersion and low-dissipation explicit numerical schemes developed in the computational aeroacoustics community [2, 1]. Optimized finite-difference schemes and selective filters over 11 points are used for spatial derivation and grid-to-grid oscillations removal, respectively. These schemes allow to accurately calculate acoustic wavelengths down to five or six times the spatial mesh size. For the interior points, which are the ones separated by at least five points from the boundary, the centered fourth-order finite-difference scheme of Bogey and Bailly [2004] and the centered sixth order selective filter of Bogey et al. [2009] are used. For the boundary which are the five extreme points in each direction, the eleven-point non-centered finite-difference schemes and selective filters of Berland et al. [2007] are chosen. The optimized six-stage Runge-Kutta algorithm proposed by Bogey and Bailly [2004] is used for time integration.

The time-domain impedance boundary condition described in [4] is applied at the liner location. The radiation boundary conditions of Tam and Dong [13] are implemented at the others boundaries. They are applied to the last five rows at each boundary points. The inlet and outlet sections are assumed to be anechoic and are implemented as damping zones, including non-reflecting boundary conditions.

2.2 Broadband time-domain impedance boundary condition.

In this work, a broadband impedance eduction method is developed instead of determining the surface impedance for each frequency of interest. A broadband formulation must provide an interpolation and an extrapolation of the surface impedance outside of the specified range of frequencies. A natural approach is to seek an expression of the surface impedance as a rational function

$$Z(\omega) = \frac{a_0 + \dots + a_N(-i\omega)^N}{1 + \dots + b_N(-i\omega)^N}. \quad (3)$$

This form offers two main advantages. Firstly, a recursive algorithm can be used which permits an efficient computation of the convolution in the time domain. Secondly, the coefficients can be chosen to guarantee the impedance to be physically admissible [11]. Using a partial fraction decomposition, the rational function can be written as

$$Z(\omega) = Z_\infty + \sum_{k=1}^P \frac{A_k}{\lambda_k - i\omega} + \sum_{k=1}^S \left(\frac{B_k + iC_k}{\alpha_k + i\beta_k - i\omega} + \frac{B_k - iC_k}{\alpha_k - i\beta_k - i\omega} \right) \quad (4)$$

where $[Z_\infty, A_k, B_k, C_k] \in \mathbb{R}$ and $[\lambda_k, \alpha_k, \beta_k] \in \mathbb{R}^+$. With this form the impedance is always causal and satisfies the reality condition. The passivity condition $\text{Re}[Z(\omega)] > 0$ has to be checked for each set of the coefficients. In the present approach, the characteristic impedance $Z(\omega)$ is approximated using only two pairs of complex conjugate poles, i.e. $P = 0$ and $S = 2$. The eduction method proposed in the next section aims in determining the nine coefficients of the impedance model.

3 Multiobjective optimization for the impedance eduction

Iterative impedance eduction methods provide an estimate of the acoustic impedance by minimizing the error between the numerically calculated and the measured sound pressure along the duct. The choice of the minimization method have to be made taking into consideration following items. First, the broadband model of acoustic propagation under a grazing flow gives the possibility to take into account all studied frequencies at once. Second, the broadband impedance model is fully determined by nine coefficients, so there are nine independent design variables in the optimization problem. These two elements bring us to the multiobjective optimization procedure with the help of the

genetic algorithm NSGA-II. The non-dominated solutions of the optimization process, i.e. solutions that cannot be improved in any of the objectives without degrading at least one of the other objectives, form a Pareto front. The corresponding optimization problem reads

$$\begin{aligned}
 \min \quad & f_i(Z(\mathbf{X})) = \sum_{l=1}^L (P_l|_{\text{NASA}} - P_l|_{\text{FDTD}}) (P_l^*|_{\text{NASA}} - P_l^*|_{\text{FDTD}}) \\
 \text{such that} \quad & \underline{x}_j \leq x_j \leq \overline{x}_j, ; \quad \mathbf{X} \in \mathbb{R}^n \\
 & \text{Re}(Z(\mathbf{X})) > 0, \\
 \text{with} \quad & i = 1..n, \quad n \text{ is the number of objective functions} \\
 & j = 1..m, \quad m \text{ is the number of design variables}
 \end{aligned} \tag{5}$$

where f_i are the objective functions, \mathbf{X} are the design variables that are the coefficient of broadband impedance model Z , $P_j|_{\text{NASA}}$ is the complex pressure values obtained from the measurements of Jones et al. [2005] and $P_l|_{\text{FDTD}}$ is the complex pressure values obtained from the results of numerical simulations for microphone positions l . The symbol $*$ is used to denote the complex conjugate. Constrained conditions on x_j correspond to the constraints on the broadband impedance model coefficients $Z_\infty, B_k, C, \alpha_k$ and β_k .

The next step performs robust optimization using the non-dominated sorting genetic algorithm NSGA-II.

4 Validation of the method

4.1 Measurements setup and simulation parameters

The liner impedance eduction method is examined in a simplified geometry configuration. A sketch of the three-dimensional flow duct is presented in Figure 1. It corresponds to the geometry of the duct studied in [7], which provided a reference data set for validation of impedance eduction codes.

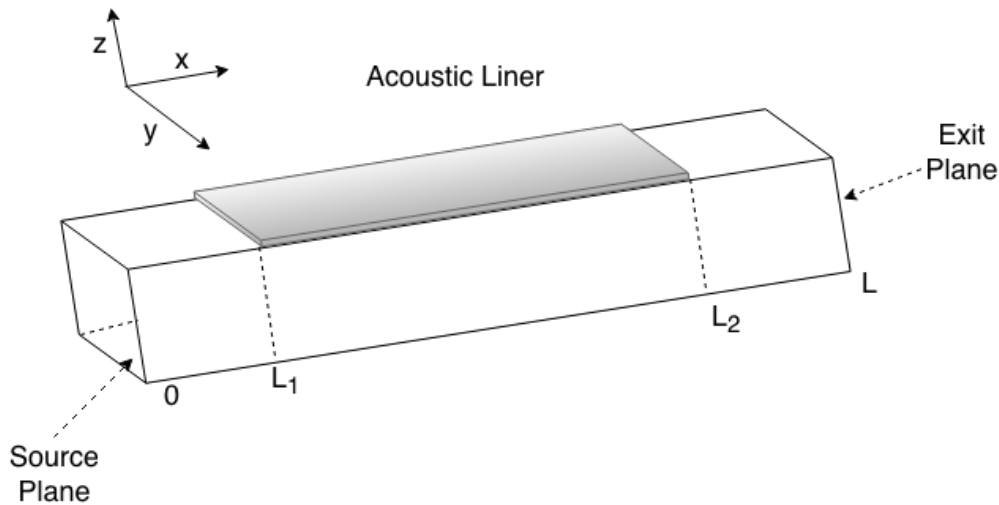


Figure 1: Sketch of the NASA Langley Grazing Flow Impedance Tube [7]

The source and the exit planes of the computational area are located at $x = 0$ and $x = L$, respectively. The lower and two-side walls are rigid. The upper wall is also rigid except of the region when $x \in [L_1; L_2]$, which contains the liner, the internal dimensions of the duct are $[L_y \times L_z]$, with $L = 0.812$ m, $L_1 = 0.203$ m, $L_2 = 0.609$ m, $L_y = L_z = 0.051$ m. A ceramic tubular liner was used for this study. This liner provides an impedance spectrum that varies over a range typically observed in aircraft engine nacelle liners. It consists of parallel, cylindrical channels embedded in a ceramic matrix.

In NASA measurements, data was acquired with 31 microphones mounted flush to the wall opposite the liner. Three microphones were located upstream of the liner, three microphones were located downstream, and the other 25 microphones were located in the lined section. Six of these microphones were chosen for the eduction method, situated at $x = [0.1; 203.3; 330.3; 431.9; 584.3; 812.9]$ mm.

A parabolic mean velocity profile is considered for the 2D model of the duct. The computational area is discretized by

500 × 26 points with the uniform spatial step $\Delta x = \Delta y = 4.17 \times 10^{-3}$ m. The simulation is run up to $t_{max} = 0.014$ s with the step of $\Delta t = 1 \times 10^{-5}$ s. The computational time is 8 s on the desktop computer for single TDFD simulation. The simulation is initialized as follows:

$$\begin{aligned} \mathbf{v}(\mathbf{x}, t = 0) &= \mathbf{0} \\ p(\mathbf{x}, t = 0) &= \rho_0 c_0^2 \exp(-\ln(2) \frac{x^2}{B^2}) \end{aligned} \quad (6)$$

with the gaussian half-width set to $B = 5\Delta x$. The pressure is calculated by Fourier transform of the time-domain solution to the frequency domain.

For the optimization procedure, 26 frequencies are considered, $f \in [500; 3000]$ Hz, that provides $n = 26$ objective functions. Nine design variables that correspond to the coefficients of the impedance formulation are considered. Education was conducted for Mach number $M = [0; 0.079; 0.255; 0.335]$, based on the bulk velocity.

4.2 Results

Impedance education results for $M = 0$ and $M = 0.335$ are presented in Figure 2. Pressure measurements for 26 frequencies from 500 Hz to 3000 Hz are used. The educed impedance is on good agreement with the results presented by NASA over the whole frequency band of interest, with or without the presence of the flow.

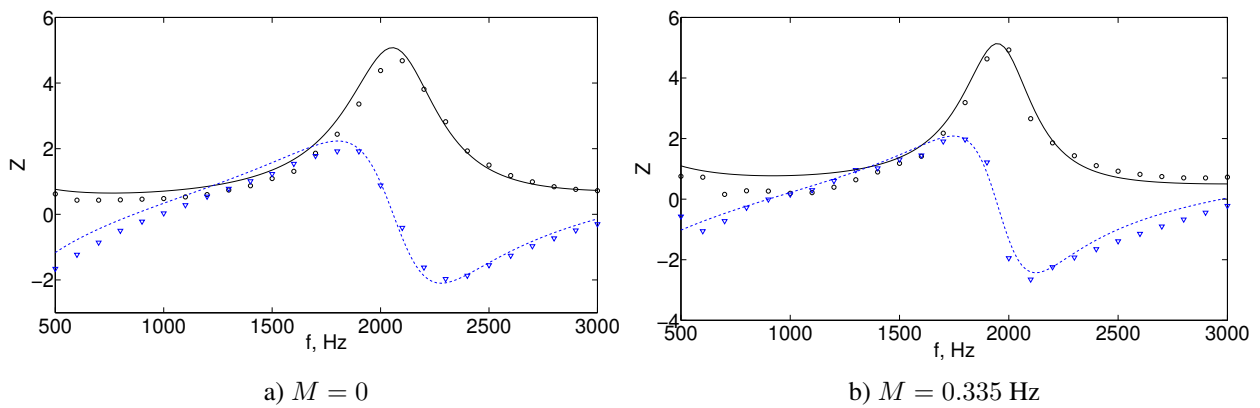


Figure 2: Real (black solid line) and imaginary (blue dashed line) parts of the educed impedance in the NASA grazing incidence tube as a function of the frequency obtained using the LEEs solver. Corresponding NASA results are marked by circles and triangles.

Accuracy of the results is provided by two issues. First, an appropriate number of elements must be chosen in each generation during the optimization cycle. Second, a sufficiently large number of frequencies have to be considered. Tests with smaller quantity of frequencies, and consequently smaller quantity of objective functions were conducted, and showed that the more frequencies are used, the better results are obtained. The same behavior was observed for other Mach numbers.

5 Conclusion

An impedance education method for the identification of the impedance characteristics of the acoustic liner in the duct under the grazing flow has been developed. The broadband simulation model formulated in the time domain is found to be efficient in the terms of computation time and robustness of the results. The genetic optimization algorithm NSGA-II has been used for education itself. This method has been validated using the experimental data provided by NASA measurements [7].

6 Acknowledgment

This research was carried out on behalf of the European project ENOVAL. The authors also would like to thank Dr. Michael Jones (NASA) for providing the benchmark data.

References

- [1] Berland, J., Bogey, C., Marsden, O., and Bailly, C. (2007). High-order, low dispersive and low dissipative explicit schemes for multiple-scale and boundary problems. *Journal of Computational Physics*, 224(2):637–662.
- [2] Bogey, C. and Bailly, C. (2004). A family of low dispersive and low dissipative explicit schemes for flow and noise computations. *Journal of Computational Physics*, 194(1):194–214.
- [3] Bogey, C., De Cacqueray, N., and Bailly, C. (2009). A shock-capturing methodology based on adaptative spatial filtering for high-order non-linear computations. *Journal of Computational Physics*, 228(5):1447–1465.
- [4] Dragna, D., Cotté, B., Blanc-Benon, P., and Poisson, F. (2011). Time-domain simulations of outdoor sound propagation with suitable impedance boundary conditions. *AIAA Journal*, 49(7):1420–1428.
- [5] Elnady, T., Bodén, H., and Elhadidi, B. (2009). Validation of an inverse semi-analytical technique to educe liner impedance. *AIAA Journal*, 47(12):2836–2844.
- [6] Eversman, W. and Gallman, J. M. (2011). Impedance eduction with an extended search procedure. *AIAA Journal*, 49(9):1960–1970.
- [7] Jones, M. G., Watson, W. R., and Parrott, T. L. (2005). Benchmark data for evaluation of aeroacoustic propagation codes with grazing flow. *AIAA paper*, 2853:2005.
- [8] Primus, J., Piot, E., and Simon, F. (2013). An adjoint-based method for liner impedance eduction: Validation and numerical investigation. *Journal of Sound and Vibration*, 332(1):58–75.
- [9] Reymen, Y., Baelmans, M., and Desmet, W. (2008). Efficient implementation of Tam and Auriault’s time-domain impedance boundary condition. *AIAA Journal*, 46(9):2368–2376.
- [10] Richter, C., Hay, J. A., Schönwald, N., Busse, S., Thiele, F., et al. (2011). A review of time-domain impedance modelling and applications. *Journal of Sound and Vibration*, 330(16):3859–3873.
- [11] Rienstra, S. W. (2006). Impedance models in time domain, including the extended helmholtz resonator model. *AIAA paper*, 2686:2006.
- [12] Sellen, N., Cuesta, M., and Galland, M.-A. (2006). Noise reduction in a flow duct: Implementation of a hybrid passive/active solution. *Journal of sound and vibration*, 297(3):492–511.
- [13] Tam, C. K. and Dong, Z. (1996). Radiation and outflow boundary conditions for direct computation of acoustic and flow disturbances in a nonuniform mean flow. *Journal of Computational Acoustics*, 4(02):175–201.
- [14] Watson, W., Jones, M., Tanner, S., and Parrott, T. (1996). Validation of a numerical method for extracting liner impedance. *AIAA Journal*, 34(3):548–554.